IEEE Access
Multidisciplinary | Rapid Review | Open Access Journal

Received July 5, 2018, accepted August 6, 2018, date of publication August 21, 2018, date of current version October 12, 2018.

Digital Object Identifier 10.1109/ACCESS.2018.2866482

A Miniaturized Base Station Antenna With Novel Phase Shifter for 3G/LTE Applications

YEJUN HE[1], (Senior Member, IEEE), JUN LI[1], SAI WAI WONG[1], (Senior Member, IEEE), XIAOFANG PAN[1], LONG ZHANG[1], AND ZHI NING CHEN[2], (Fellow, IEEE)

[1]College of Information Engineering, Shenzhen University, Shenzhen 5186060, China
[2]Department of Electrical and Computer Engineering, National University of Singapore, Singapore 119077

Corresponding author: Yejun He (heyejun@126.com)

This work was supported in part by the National Natural Science Foundation of China under Grant 61372077, Grant 61801299, and Grant 61871433, in part by the Shenzhen Science and Technology Programs under Grant ZDSYS 201507031550105, Grant JCYJ20170302150411789, Grant JCYJ20170302142515949, and Grant GCZX2017040715180580, in part by the Guangzhou Science and Technology Program under Grant 201707010490, and in part by the Guangdong Provincial Science and Technology Program under Grant 2016B090918080.

ABSTRACT This paper presents a new type of miniaturized base station antenna array, which consists of a metal reflector, six upper-band dipoles, and a couple of ladder sidewalls, operating over 1.71–2.69 GHz (DCS/PCS/UMTS/LTE). Meanwhile, this paper also proposes a novel miniaturized phase shifter with one input and five outputs to enable the antenna array to achieve electrical downtilt (0°–10°) in the operating frequency band. Three different sidewalls are applied in the proposed antenna array to compare their performance. Simulated results demonstrate that the antenna array with ladder sidewalls can achieve an excellent performance, and this proposed phase shifter also has good electrical properties to help the proposed antenna array realize downtilt. The proposed antenna array and phase shifter are fabricated and measured, and the measured results show that the antenna array has good radiation characteristics, including low-voltage standing wave ratio (< 1.4), high port-to-port isolation (>31 dB), low third-order passive intermodulation ($_3 < -120$ dBm), stable radiation patterns with horizontal half-power beamwidth $65° \pm 5°$, high front-to-back ratio (> 30 dB), and high cross-polarization discrimination at $\pm 60°$ azimuth (>11.5 dB) in all frequency bands and electrical downtilt angles. The proposed antenna array exhibits an acceptable gain of 15 ± 1.1 dBi across the operational frequency band.

INDEX TERMS Antenna array, phase shifter, broadband, miniaturized.

I. INTRODUCTION

In recent years, with the continuous development of mobile communication systems, 2G, 3G and 4G will co-exist for a long time. Moreover, there is a growing demand for broadband antennas that can serve multiple systems at the same time because the site resources gradually reduce. Since dual-polarized base station antenna arrays can provide polarization diversity to increase system capacity and combat the problem of multipath fading [1], they are also widely used.

For the above reasons, different multiband dual-polarized base station antenna arrays have been studied [2]–[8]. In [2]–[4], some broadband dual-polarized base station antennas have been developed to meet the market demand, while their bandwidths are not enough to cover multi-band systems. Although a novel omnidirectional base station antenna was proposed [5], its gain can not meet the requirement of dense area. A broadband ±45° dual-polarized antenna operating in the 1.7-2.7 GHz was proposed [6], and the base station antenna array with five elements achieved a wide bandwidth. However, the isolation of antenna array can not be greater than 28 dB in the whole frequency band, which does not meet the requirements of modern base station applications. Although the broadband planar antenna array was also developed to achieve better performance [7], [8], the overall length is too long to realize the requirements for miniaturization of base station antenna array. Furthermore, the characteristic of the electrical downtilt is also the important one of the base station antenna array [9], because it can easily steer the main lobe coverage area of an antenna array and has little influence on radiation pattern. However, the design of base station antennas in many literatures have not electrical downtilt function [3], [7], [10]. In [8] and [11],

the base station antenna array with electrical downtilt can get better performance, but none of them can clearly explain how to achieve downtilt of the antenna array. The key to realize electrical downtilt is the use of phase shifter, which enables the direction of vertical beam of antenna array to be steered [12]. On the other hand, the big volume problem of multi-system antenna becomes the main problem in the network construction of the common site. The application of miniaturized technology solves this problem to some extent, and one of the miniaturized technology is to reduce the overall size of the antenna array by using fewer elements [6], [13]. However, the antenna arrays can not be used in modern base station construction due to their less port isolation or gain.

In this paper, a novel broadband and dual-polarized antenna array for 1.71 GHz-2.69 GHz applications is designed. The proposed antenna array has the characteristics of miniaturization, which reduces the overall size and has the appropriate gain by using six antenna elements. The antenna array has also the function of electrical downtilt by designing a novel miniaturized phase shifter, which can manipulate the phase of each element. In addition, three different structures of sidewalls are compared to improve the radiation performance of the antenna array, including half-power beam width, gain, cross-polar discrimination (XPD)(0° and ±60°). After optimization and fabrication, a compact size of 660 mm × 145 mm × 34 mm and excellent electrical performance are achieved.

II. ANTENNA DESIGN AND DISCUSSION

A. DESIGN OF ANTENNA ARRAY

In this section, the novel antenna array is proposed. In the array design, the element we proposed [14] is applied to the proposed antenna array as shown in Fig. 1, which consists of two crossed-dipoles, two couple of baluns and a pair of inverted L shape feeding strips [15]. Compared with traditional square-loop dipole, the impedance bandwidth of the element can be greatly improved by employing parasitic metal stubs and branches [14]. As shown in Fig. 2, experiments illustrate that the element matches well in the frequency band from 1.7 to 2.7 GHz with the low voltage standing wave ratio (VSWR<1.5) and it has a relatively stable antenna gain of 8.5 ± 0.4 (dBi). What is more, the element has great port isolation with more than 30 dB and stable radiation pattern with half-power beam width (HPBW) 65.2° ± 5.6° at

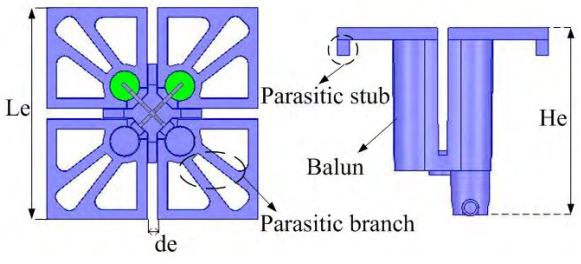

FIGURE 1. The top view and side view of the element.

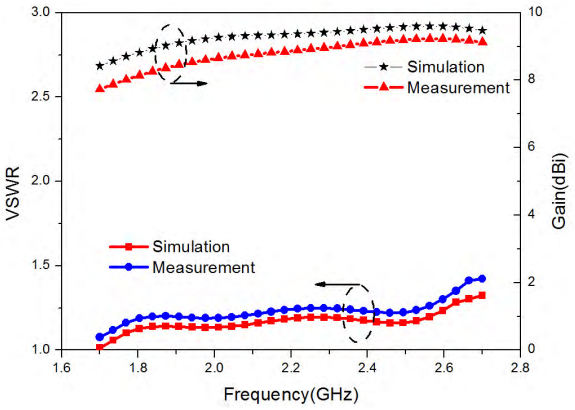

FIGURE 2. Simulated and Measured VSWRs and gains of the antenna element.

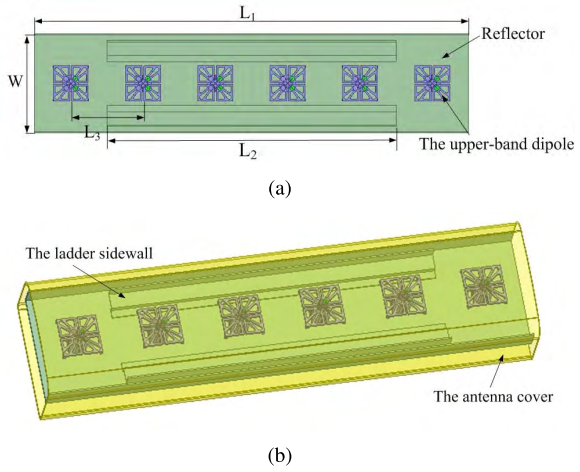

FIGURE 3. Simulated model of the proposed antenna. (a) top view. (b) 3D antenna array.

H-plane. Because of the above reasons, the antenna element is used to assemble a miniaturized antenna array with six elements. The configuration of the proposed antenna array is shown in Fig. 3, which consists of a rectangular reflector, six elements, and a pair of ladder sidewalls, where L_1 is the length of antenna array, L_2 is the length of the sidewall, and L_3 is the spatial distance between two adjacent elements.

We know that the distance between adjacent elements is related to the wavelength of the frequency, and antenna gain also increases with the increase of distance [11]. At the same time, in order to avoid the emergence of the grating lobe, and the distance between elements is smaller than the wavelength of operating frequency band. The proposed antenna array operates in the frequency band of 1.71-2.69 GHz with the wavelength from 110 mm to 175 mm. In order to obtain higher gain and inhibition of gate valve, the distance between adjacent elements is 110 mm.

On the other hand, this paper proposes three different structures of sidewalls to improve the radiation performance of the proposed antenna array. As shown in Fig. 4, it is a lateral view of three structures, (A) is the ladder sidewall, (B) is the

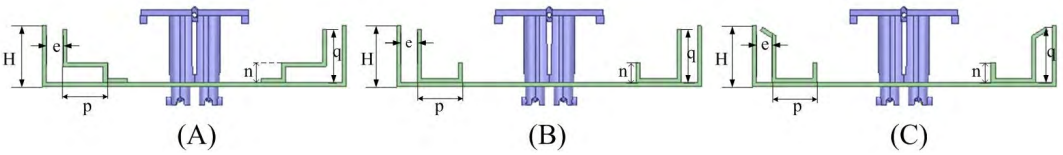

FIGURE 4. Three different structures of sidewalls. (A) The ladder sidewall (B) The u-shaped sidewall (C) The slanted sidewall.

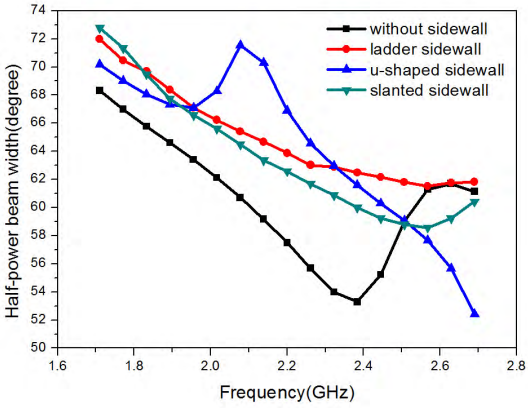

FIGURE 5. The simulated HPBW of antenna arrays with three structures of sidewalls and without sidewall.

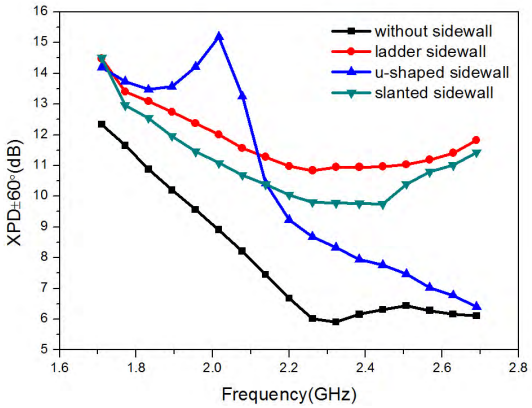

FIGURE 6. The simulated XPD (±60°) of antenna arrays with three structures of sidewalls and without sidewall.

u-shaped sidewall, and (C) is the slanted sidewall. For easily comparing the features of these sidewalls, they are set to the same height q and width p, and the distance to the side of the reflector is the same as the distance e, as well as the same length n of stub of sidewalls. Then, the working effects of the proposed antenna is analyzed with the aid of simulated results obtained using HFSS16. As shown in Fig. 5, antenna arrays with three different sidewalls are compared with that without sidewalls, and the results show that antenna arrays with sidewalls will change the half-power beam width (HPBW). The HPBW range of antenna array without sidewalls is larger from 53° to 69°, and the antenna array with ladder sidewalls and the one with slanted sidewalls have good performance, which can maintain HPBW between 60° to 72°. It can be seen that the proposed antenna with ladder sidewalls or slanted sidewalls is a good choice to achieve stability and convergence of HPBW.

In addition, the XPD at ±60° azimuth has not been mentioned in many literatures [5]–[8], but it is very important in modern base station communication applications. In this paper, the XPD (±60°) is also compared to select the most appropriate sidewall. From Fig. 6, we can know that the XPDs (±60°) of the antennas with sidewalls are better than one without sidewalls in all the operating frequency band, and the antenna with ladder sidewalls keeps relatively stable and larger XPD values from 11 dB to 15 dB compared to the other two antennas with u-shaped sidewalls and slanted sidewalls, which can meet the communication requirements. As shown in Fig. 7, we can also see that the gain results of the antennas with and without sidewalls. The results show

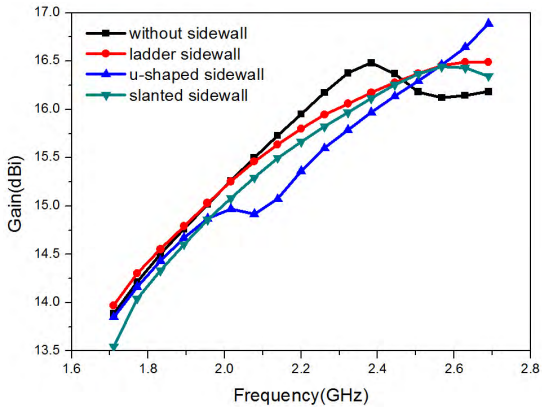

FIGURE 7. The simulated gains of antenna arrays with three structures of sidewalls and without sidewall.

that the antennas with ladder sidewalls and slanted sidewalls have good performance, where the gain increases with the increase of frequency. Although the gains are higher in some frequency bands for the other antenna arrays with u-shaped sidewalls and without sidewalls, their gains have fluctuation in the entire frequency band. It can be seen in more detail that the antenna with ladder sidewalls has a higher gain than the antenna with slanted sidewalls. After comparing the HPBW, gain and XPD (±60°) of four antenna arrays, we select the ladder sidewall to design the proposed antenna array.

Furthermore, the length of ladder sidewall (L_2) can still be optimized to further improve the performance of the antenna. As shown in Fig. 8, the HPBW range of the antenna is much

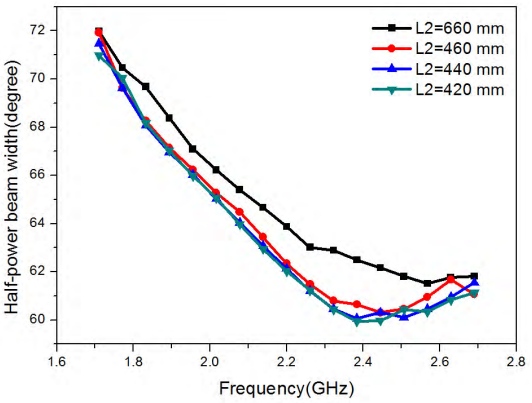

FIGURE 8. The variations of HPBW in H-plane under different L_2.

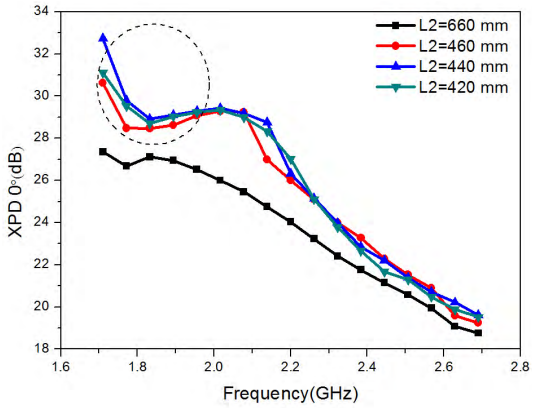

FIGURE 10. The variations of XPD (0°) under different L_2.

reduced from 71° to 60° with the increase of the frequency when the length of L_2 increases from 420 mm to 460 mm, which is obviously better than one when the length of L_2 is 660 mm. However, when L_2 increases from 420 mm to 460 mm, the HPBW range of variation is roughly the same, so it is difficulty to confirm which length of L_2 is the best. In order to further confirm the optimal length of L_2, front-to-back ratio (FBR) and XPD at the boresight direction (0°) are also chosen to compare.

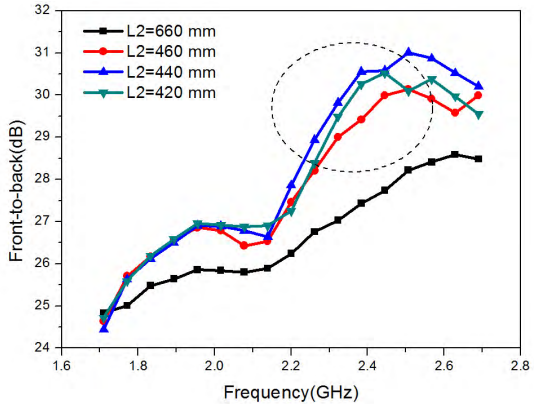

FIGURE 9. The variations of FBR under different L_2.

Fig. 9 shows the simulated results of FBR with different lengths of L_2. It can be seen that the range of FBR changes from 24 dB to 31 dB when L_2 changes from 420 mm to 460 mm, which is significantly better than one when the length of L_2 is 660 mm. What is more, when L_2 is 440 mm, the FBR in the lower frequency band is almost the same compared with other cases (420 mm and 460 mm) but FBR is relatively higher in the upper frequency band.

Fig. 10 also shows that responses of cross-polar discriminations (0°) with different lengths of L_2. Although XPDs change a little when L_2 increases from 420 mm to 460 mm, three cases are still better than one when the length of L_2 is 660 mm. In the dotted circle of Fig. 10, the proposed antenna array with the 440 mm of L_2 is slightly higher than others. It has a superior data from 20 dB to 32 dB in the working frequency band, which meets the requirements of cross-polar discrimination at the boresight direction in modern communications.

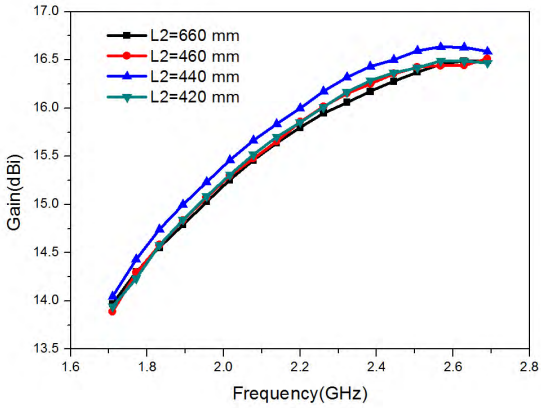

FIGURE 11. The variations of gain under different L_2.

Fig. 11 depicts variations of gains with different lengths of L_2. It is obviously that the gain is relatively higher when L_2 is 440 mm than other cases. Simulated results show that the gain of the proposed antenna array can be from 14 dBi to 16.5 dBi in the entire frequency band, which is higher than antenna arrays in other literatures [6], [10], [13].

As mentioned above, the optimum length of the ladder sidewall of the proposed antenna array is 440 mm. Specific parameters of the proposed antenna array are optimized and also displayed in Table 1.

TABLE 1. Detailed values of the proposed antenna array.

Parameter	Value	Parameter	Value	Parameter	Value
Le	53 mm	de	2.7 mm	He	47 mm
L_1	660 mm	L_2	440 mm	W	145 mm
L_3	110 mm	H	30 mm	e	8 mm
p	22 mm	n	10 mm	q	26 mm

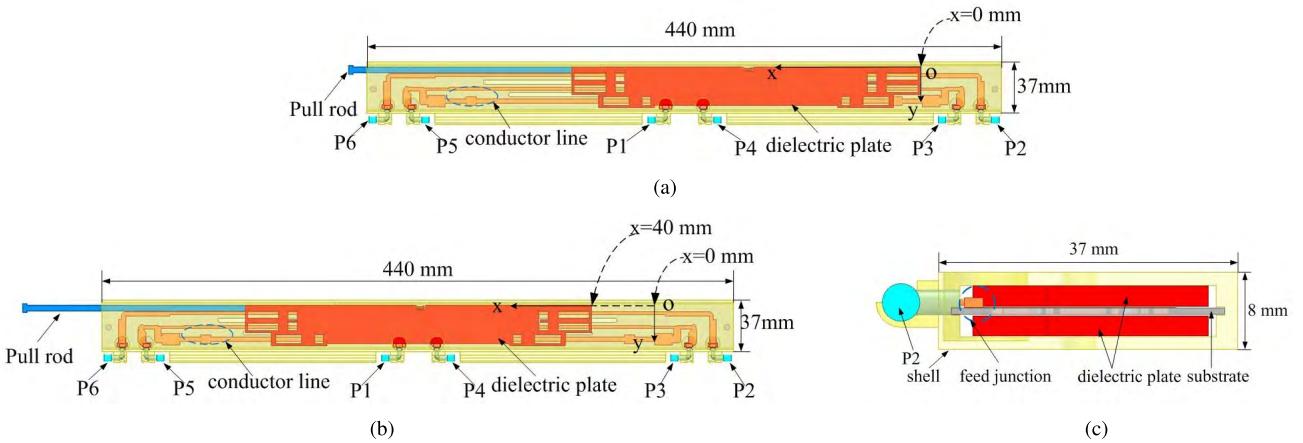

FIGURE 12. The simulated model of phase shifter. (a) Top view of phase shifter, x = 0 mm. (b) Top view of phase shifter, x = 40 mm. (c) Sectional view of phase shifter.

B. DESIGN OF PHASE SHIFTER

In this section, the miniaturized phase shifter is designed where the phase shifter belongs to the type of dielectrics moving longitudinally. As shown in Fig. 12, this is the simulated model of the proposed phase shifter, which consists of a shell, a substrate ($\varepsilon_r = 2.5$) and two dielectric plates, and two conductor lines are placed on the substrate to form a feed network. The power distribution on the port is realized by the feed network. As shown in Fig. 12(a)(b), the pull rod outside the shell is used to move the pair of dielectric plates to the left. Therefore, the function of this miniaturized phase shifter is that the VSWR and power distribution ratio can be guaranteed when the dielectric plate is moved to the left, and sufficient phase change can also be obtained to meet the requirements of the downtilt angle of the proposed antenna array.

When the electromagnetic wave passes through the stripline of length L, the phase delay (ϕ) generated is:

$$\phi = \frac{2\pi L * \sqrt{\varepsilon_r}}{\lambda_0} \tag{1}$$

where λ_0 is the wavelength of the working frequency, and ε_r is the equivalent permittivity.

It's known from the equation (1) that the change of signal transmission phase can be realized by changing the length of transmission line and the permittivity. Since changing permittivity of the stripline can achieve phase shift [16], the basic principle of the proposed phase shifter is to change the equivalent permittivity of the stripline. As shown in Fig. 12(a), the phase shifter has one input and five output with dielectrics moving longitudinally. P1 is the input port, and P2, P3, P4, P5, P6 are the output ports. The proposed phase shifter operates based on the following principle: the thickness of the covered stripline will be changed when the dielectric plate is moved so that different equivalent permittivity can be obtained. When the dielectric plate is in original position (x = 0 mm), the angle of downtilt is 0°.

In order to achieve the angle downtilt of vertical beam, the feeding phase difference (dϕ) of two radiation adjacent elements is required:

$$d\phi = \frac{2\pi f * L_3 * sin\theta}{c_0} \tag{2}$$

where the distance between adjacent elements of the proposed antenna array is L_3, f is the operating frequency, c_0 is the speed of light, and θ is the angle of downtilt.

The proposed phase shifter uses a material with a permittivity of 3.8 as the dielectric plate. Because the distance between elements of the proposed antenna array is 110 mm, the phase difference can be obtained by the equation (2) of adjacent elements for 50 degrees when f is 2.2 GHz and downtilt is set to 10 degrees. Thus the phase difference between two phase shifter ports is 50 degrees, and the moving distance of 40 mm can be obtained by the equation (1), which can meet the requirement of phase change. In Fig. 12(a), the dielectric plate is in initial state when x is 0 mm. As shown in Fig. 12(b), when the dielectric plate moves to the left, the x = 40 mm means that the moving distance is 40 mm, which represents the 10° of downtilt angle.

In order to make the antenna have smaller sidelobe, the power ratio of each port of the phase shifter needs to be reasonably allocated, so the power ratio of the phase shifter proposed in this paper is set to P6: P5:P4: P3: P2 = 1:2:3:2:1 with reference to the Taylor distribution [17]. In the design of feed network, the conductor lines are designed and fabricated on a substrate with a permittivity of 2.55, and a thickness of 0.8 mm. The circuit schematic diagram of this feed network is shown in Fig. 13, the power distribution is realized by using multi-node impedance transformation and multi-section power divider [18], [19]. In general, T-junction power divider can realize power distribution of any proportion. We assume that the transmission line is lossless, the impedance of input port is Z_0, and the characteristic impedance of the two output ports are Z_1 and Z_2 respectively. Thus the power ratio of the output port is:

$$\frac{P_1}{P_2} = \frac{Z_2}{Z_1} \tag{3}$$

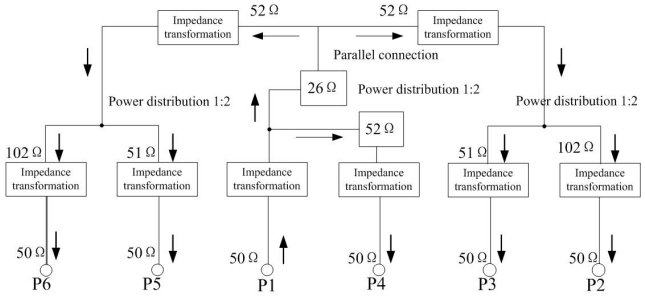

FIGURE 13. The overall structure of the feed network.

where P_1 represents the power of output port 1, P_2 represents the power of output port 2.

As shown in Fig. 13, P1 serves as the energy input port while other ports are the output ports. The energy flow is shown in the arrow in the figure. In addition, the characteristic impedance of transmission line can be changed by changing the width of lines, so impedance transformation can be achieved by changing the width of some branch lines in the feed network. When the energy passes through P1 port, it reaches the first T-junction power divider after impedance transformation. In the first T-junction power divider, the first section of the transmission line has a characteristic impedance of 52 Ω while the second section has a parallel impedance of 26 Ω, which can achieve a 1:2 power distribution by equation (3). On the branches of P5 and P6 ports, the characteristic impedance of the branch is 52 Ω. After the impedance transformation, a T-junction power divider is used to achieve power distribution. Since the characteristic impedance of the P5 branch line is 51 Ω while P6 section has a characteristic impedance of 102 Ω, another 1:2 power distribution can be obtained. Additionally, the branches of P3, P2 and P5, P6 are symmetric, the power distribution ratio of the branches of P3 and P2 is 1:2. Therefore, the total power distribution of the feed network is P6: P5:P4: P3: P2 = 1:2:3:2:1.

In addition, the phase shift of port P4 can be considered to be approximately constant when the phase shifter works, and port P4 can be set to fixed port. Thus the ratio of phase shift of other ports relative to port P4 can be set to θ_6:θ_5:θ_3:θ_2 = 2 : 1 : 1 : 2, which can ensure that phase shift between adjacent ports is consistent when the phase shifter works. The average phase shift of each output port θ_{ave} is given by:

$$\theta_{ave} = \frac{0.5 * |\theta_6| + |\theta_5| + |\theta_3| + 0.5 * |\theta_2|}{n} \tag{4}$$

where θ_6, θ_5, θ_3, θ_2 are phase shift of output ports of P6,P5,P3,P2 relative to P4.

As shown in the Fig. 14, the simulation results show that when the dielectric plate is in two states (x = 0 mm and x = 40 mm), the VSWRs of the input port P1 are still below 1.3, which is beneficial to the designment of the proposed antenna array. In addition, the impedance of each branch will fluctuate in the process of moving dielectric plate,

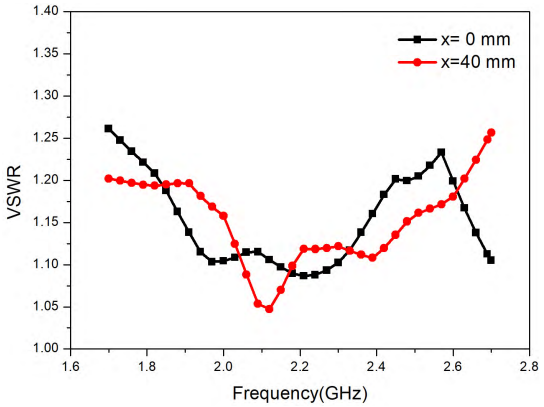

FIGURE 14. The simulated VSWR of phase shifter.

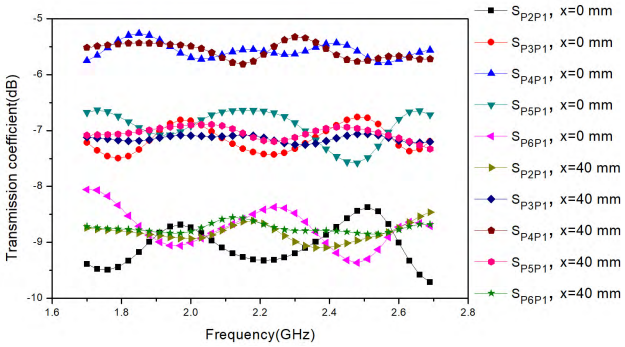

FIGURE 15. The simulated transmission coefficient of phase shifter.

which affects the output power of each port, but simulation results of transmission coefficient (Fig. 15) show that the transmission coefficient fluctuation of each port is less than 1dB, so it can satisfy the designment of the proposed antenna array in practice.

The loss is also an important index of the phase shifter. The gain of the antenna array loaded with the phase shifter will be reduced when the loss of the phase shifter is too large. The phase shifter designed in this paper is a multi-port device, so the loss of the phase shifter can be obtained by subtracting the reflection energy of incident port P1 and the transmission energy of other received ports (P2, P3, P4, P5, P6) through the total energy. The loss is given by:

$$Loss = 10\log_{10}(1 - |S_{P1P1}|^2 - |S_{P2P1}|^2 - \ldots - |S_{PnP1}|^2) \tag{5}$$

where $Loss$ stands for loss of phase shifter, S_{P1P1} is reflection coefficient of P1 port, and S_{PnP1} represents the transmission coefficient from P1 port to Pn port, n is 2, 3, 4, 5, 6.

III. MEASURED RESULTS AND PERFORMANCE ANALYSIS

In order to verify the effectiveness of the antenna array, the prototype of the antenna array with miniaturized phase shifter is fabricated and experimentally tested. The configuration of the antenna array is shown in Fig. 16, where the front

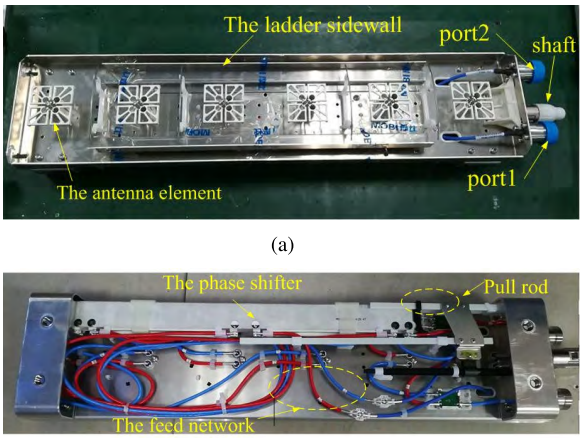

FIGURE 16. Prototype of the proposed antenna array. (a) front view. (b) back view.

view is radiation elements and a pair of ladder sidewalls, and the back view is feed networks with miniaturized shift phaser. In the back view, the pull rod moves by means of rotating shaft, so the position of the dielectric plate can be adjusted to achieve the change of phase.

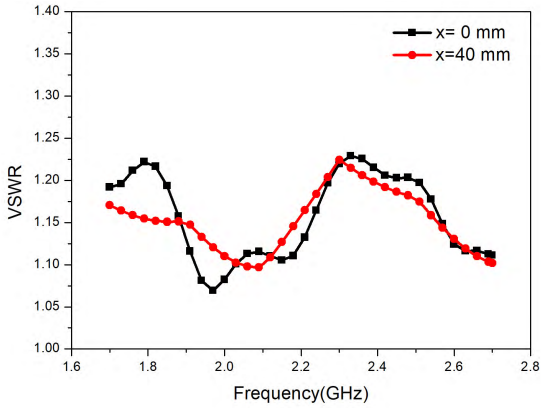

FIGURE 17. The measured VSWR of phase shifter.

First of all, the miniaturized phase shifter is measured by vector network analyzer E5071C. The measured results are shown in Fig. 17, where VSWRs are still less than 1.3, which is in agreement with the simulated results. While measured transmission coefficients (Fig. 18) are less than the results of simulated ones, the fluctuation of transmission coefficients is still not more than 1 dB, which can meet the requirements for antenna array design in practice. The discrepancy may result from fabrication errors. Fig. 19 also shows that the simulated results and measured results of the average phase shift of the phase shifter by equation (4) when the dielectric plate is moved to 40 mm. Simulated results show that the average phase shift is 53 degrees when the frequency is 2.2 GHz, which can satisfy the design of the proposed antenna array in this paper. Although the result of measured average phase

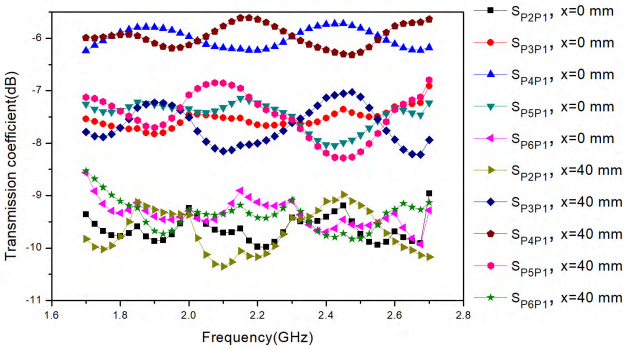

FIGURE 18. The measured transmission coefficient of phase shifter.

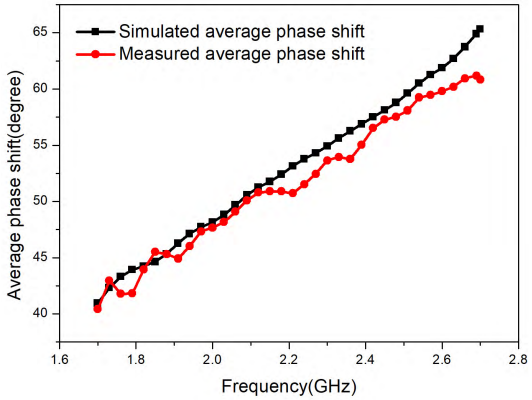

FIGURE 19. The simulated and measured average phase shift of phase shifter.

shift has a little worse than the simulated one, it still can meet the angle conditions of downtilt.

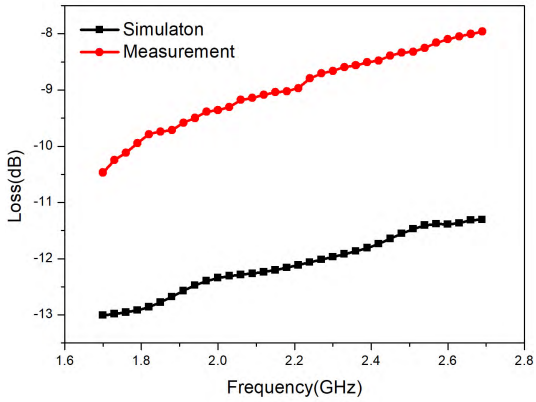

FIGURE 20. The loss of phase shifter.

In addition, the loss can be obtained through the S parameter measured in equation (5). As shown in Fig. 20, the simulation results show that the loss is between −13 dB and −11.5 dB in the entire frequency band, indicating that the phase shifter has a small loss and the energy can be transmitted with a large proportion through the phase shifter to the antenna array. It is beneficial for the gain of the antenna array.

However, the measured results show that the phase shifter has a large loss from −10.5 dB to −8 dB, but it can still be applied to the antenna array, since the antenna can obtain acceptable gain. The difference is caused by the transmission cable and production process.

The overall size of the proposed antenna array is 660 mm × 145 mm × 34 mm. The VSWR and port-to-port isolation are also obtained by vector network analyzer in an anechoic chamber, and the third passive Intermodulation (PIM_3) has been also obtained by Kaelus test equipment, while radiation patterns of the antenna array are measured by far-field test system.

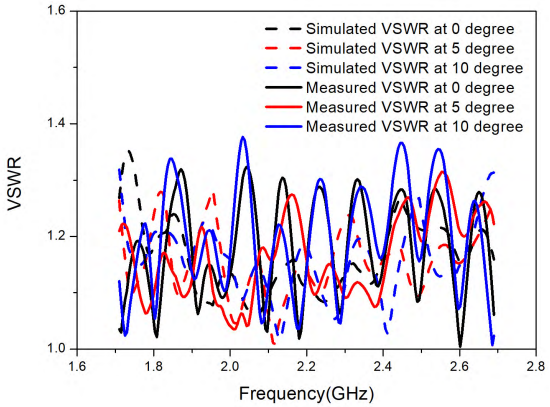

FIGURE 21. Simulated and Measured VSWR of the proposed antenna array.

Because the symmetry of the slant ±45° polarization, the result of port 1 is presented and port2 is omitted. Simulated and measured VSWRs at different downtilt angles are shown in Fig. 21. It shows that the simulated and measured VSWRs of the antenna array at 0°, 5° and 10° are less than 1.4 in the working band, which is better than more existing antenna arrays.

The simulated and measured port-to-port isolations (S_{21}) of the proposed antenna array at different downtilt angles are shown in Fig. 22. It can be seen that the maximum value of

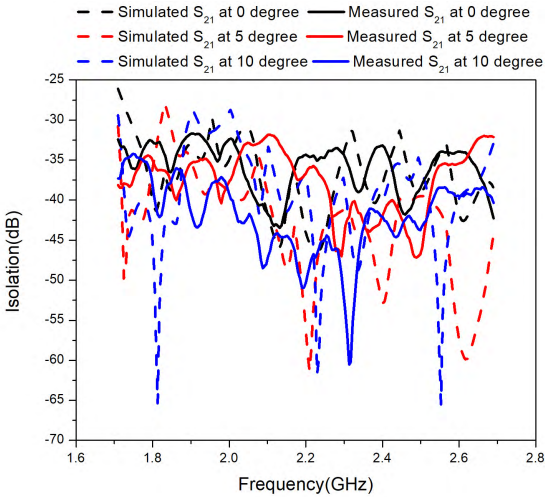

FIGURE 22. Simulated and Measured isolation of the proposed antenna array.

the simulated S_{21} of the antenna array can reach −27 dB, and measured S_{21} are less than −30 dB in all working bands and all downtilt angles. The difference between simulated results and measured ones are caused by the fabrication errors, but measured isolation of the antenna array can meet the modern communication requirements.

In addition, the proposed antenna array has also been measured for the third order passive intermodulation, which has become an important factor limiting the capacity of the communication systems. The measured results are shown in Table 2, respectively in 0°, 5° and 10° downtilt degrees both port1 and port2 at 1800 MHz, 2100 MHz, 2600 MHz. It can be seen that all the measured PIM_3 are less than −120 dBm, which is well below the −107 dBm requirements of mobile operators. Note that the proposed antenna array has good performance for communication capacity.

TABLE 2. specific results of measured the PIM_3.

Fre (MHz)	1800		2100		2600	
port	port1	port2	port1	port2	port1	port2
0°	−130.5	−127.3	−129.4	−129.8	−123.3	−122.3
5°	−131.1	−125.8	−127.9	−130.2	−124	−123.1
10°	−131.4	−128.9	−120.2	−129.8	−123.1	−122.7

Further, we use the far field test system to test the pattern of the proposed antenna array. Due to the symmetry of the structure, we measure the radiation patterns of port 1 at 1.71 GHz, 2.17 GHz, 2.69 GHz on the horizontal and vertical planes respectively, the co-polarization is −45° direction and cross-polarization is +45°, while another polarization mode is omitted. The test results of patterns are shown in Fig. 22, Fig. 23. It can be seen that the proposed antenna array has stable radiation performance.

As shown in Fig. 23, the horizontal plane radiation patterns of the co-polarization are stable (65° ± 5°) in all working frequency bands, and radiation patterns of cross-polarization will get better with the increase of frequency band. At the same time, the radiation patterns also maintains consistency at different electrical downtile angles. According to far-field test system, the specific values are obtained, such as HPBW, FBR, gain and XPD (±60°) in H-plane, which are shown in Table 3.

TABLE 3. specific results of measured radiation patterns.

Downtilt	Frequency (GHz)	HPBW (0°)	FBR (dB)	XPD ±60° (dB)	Gain (dBi)	SLS (dB)
0°	1.71	69.35	26.61	15.87	13.92	−19.35
	2.17	64.47	31.67	13.62	14.67	−19.87
	2.69	60.65	33.39	14.54	15.47	−18.58
5°	1.71	69.86	28.89	17.11	13.98	−18.03
	2.17	67.21	33.71	12.17	14.87	−19.52
	2.69	60.36	33.71	11.57	16.11	−17.56
10°	1.71	70.23	33.44	15.21	13.89	−16.94
	2.17	67.58	30.71	14.23	14.7	−16.22
	2.69	61.2	31.26	14.62	15	−17.63

It can be seen that high FBR (>26 dB) and high XPD (>11.5 dB) at ±60° azimuth are achieved at the whole

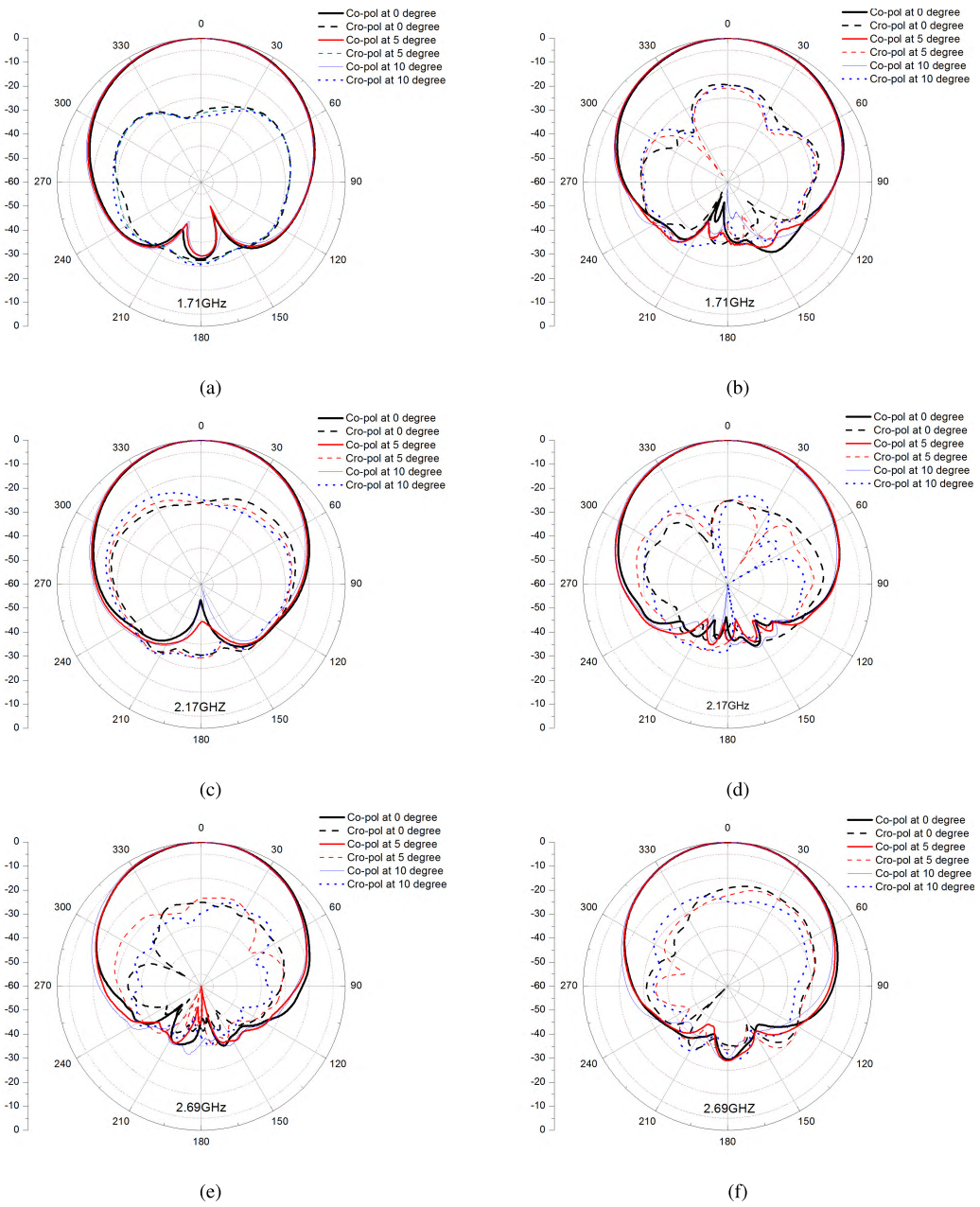

FIGURE 23. Simulated and Measured H-plane radiation patterns of the proposed antenna array. . (a) Simulated at 1.71 GHz. (b) Measured at 1.71 GHz. (c) Simulated at 2.17 GHz. (d) Measured at 2.17 GHz. (e) Simulated at 2.69 GHz. (f) Measured at 2.69 GHz.

operating bands and all downtilt angles. When the angle of electrical downtilt of the antenna beam is increased, the radiation patterns at horizontal plane are still keep stable. In Table 4, the performance of the proposed antenna array is compared with other base station antenna arrays reported in the literatures [6]–[13]. It can be seen that the proposed antenna array with six elements has excellent FBR and isolation, and the gain (15 ± 1.1 dBi) is relatively higher. What's more important is that many literatures do not consider XPD at $\pm 60^\circ$ azimuth, and the antenna array can achieve good XPD across the entire operating frequency band.

On the other hand, the vertical plane gain radiation patterns of the co-polarization at different downtilt angles are shown in Fig. 24. The definition of the first upper sidelobe suppression (SLS) is the maximum level in theta from -30° to 0°). It is obvious that the first upper sidelobe suppression in all frequency bands are below -16 dB, which meets the base station antenna array design, and it is also shown in Table 3. What is more, the downtilt angle of the main lobe can be clearly seen in the Fig. 24, which can prove the accuracy of the proposed phase shifter.

TABLE 4. Antenna's performance comparison.

Ref	Array	downtilt	Size (mm^3)	Bandwidth	Isolation	FBR	H-plane HPBW	Gain	XPD ($\pm 60°$)
[6]	5-element	electrical	600×140×34.8	1.7-2.7 GHz	>25 dB	NG	66.56°±2.22°	14.5 dBi	NG
[7]	8-element	No	NG	1.63-2.9 GHz	>25 dB	>20 dB	65°±8°	16 dBi	NG
[8]	10-element	electrical	1200×140×20	1.7-2.7 GHz	>28 dB	NG	64.85°±4.12°	> 14.23 dBi	NG
[10]	8-element	No	700×280×45	1.43-3 GHz	NG	NG	NG	14 dBi	NG
[13]	4-element	No	562.5×200×23	1.55-2.5 GHz	>35 dB	>20 dB	NG	13.5-13.9 dBi	NG
this work	6-element	electrical	660×145×34	1.71-2.69 GHz	>30 dB	>26 dB	65°±5°	15 dBi	>11.5 dB

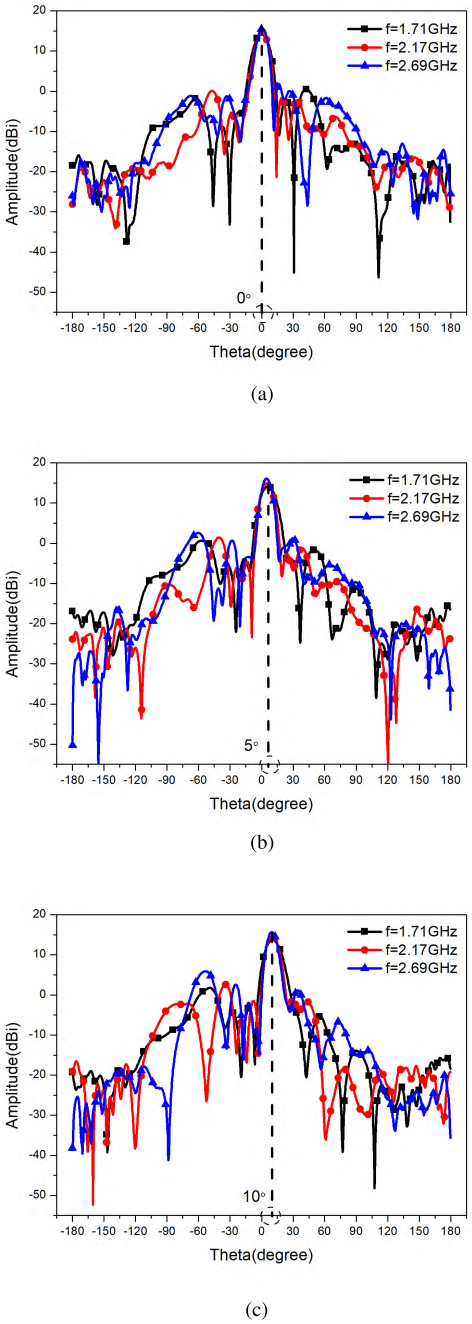

FIGURE 24. Measured V-plane gain radiation patterns of the proposed antenna array. (a) 0° downtilt. (b) 5° downtilt. (c) 10° downtilt.

IV. CONCLUSION

A novel antenna array with miniaturized phase shifter operating at 1.71 GHz-2.69 GHz has been proposed, fabricated and measured. The simulated results show that the antenna array has a better performance with ladder sidewalls than other two cases, including HPBW and XPD ($\pm 60°$), and the results of the simulation also demonstrate that the phase shifter has good electrical performance. Finally, the measurements are performed and the results show that the antenna array with miniaturized phase shifter can achieve good radiation characteristics, such as low VSWR(<1.4), high port-to-port isolation (>31 dB), and low third order passive Intermodulation ($PIM_3 < -120$ dBm). Additionally, radiation patterns show that antenna array has stable horizontal HPBW ($65° \pm 5°$), appropriate gain (15 ± 1.1 dBi), and the low SLS (<-16 dB). With these advantages, the antenna array is suitable for existing 2G/3G/LTE applications in modern mobile communication systems.

REFERENCES

[1] K. L. Wong, *Compact and Broadband Microstrip Antennas*. Hoboken, NJ, USA: Wiley, 2002.

[2] I. Seo *et al.*, "Design of dual polarized antenna for DCS, UMTS, WiBro base stations," in *Proc. IEEE Int. Conf. Wireless Inf. Technol. Syst.*, Sep. 2010, pp. 1–4.

[3] H. Huang, Z. Niu, B. Bai, and J. Zhang, "Novel broadband dual-polarized dipole antenna," *Microw. Opt. Technol. Lett.*, vol. 53, no. 1, pp. 148–150, Jan. 2011.

[4] X. Liu, S. He, H. Zhou, J. Xie, and H. Wang, "A novel low-profile, dual-band, dual-polarization array antenna for 2G/3G base station," in *Proc. IET Int. Conf. Wireless, Mobile Multimedia Netw.*, Nov. 2006, pp. 1335–1338.

[5] X. Quan and R. Li, "A broadband dual-polarized omnidirectional antenna for base stations," *IEEE Trans. Antennas Propag.*, vol. 61, no. 2, pp. 943–947, Feb. 2013.

[6] Q. X. Chu, D. L. Wen, and Y. Luo, "A broadband ±45° dual-polarized antenna with Y-shaped feeding lines," *IEEE Trans. Antennas Propag.*, vol. 63, no. 2, pp. 483–490, Feb. 2015.

[7] Y. Cui, R. Li, and H. Fu, "A broadband dual-polarized planar antenna for 2G/3G/LTE base stations," *IEEE Trans. Antennas Propag.*, vol. 62, no. 9, pp. 4836–4840, Sep. 2014.

[8] D.-Z. Zheng and Q.-X. Chu, "A wideband dual-polarized antenna with two independently controllable resonant modes and its array for base-station applications," *IEEE Antennas Wireless Propag. Lett.*, vol. 16, pp. 2014–2017, Jul. 2017.

[9] F. Athley and M. N. Johansson, "Impact of electrical and mechanical antenna tilt on LTE downlink system performance," in *Proc. IEEE 71st Veh. Technol. Conf.*, May 2010, pp. 1–5.

[10] Y. Cui, R. Li, and P. Wang, "Novel dual-broadband planar antenna and its array for 2G/3G/LTE base stations," *IEEE Trans. Antennas Propag.*, vol. 61, no. 3, pp. 1132–1139, Mar. 2013.

[11] Y. He, W. Tian, and L. Zhang, "A novel dual-broadband dual-polarized electrical downtilt base station antenna for 2G/3G applications," *IEEE Access*, vol. 5, pp. 15241–15249, 2017.

[12] S. Kan, Y. Tao, and G. Wang, "Novel dielectric wedge phase shifter for 3G mobile basestation antennas," in *Proc. Int. Conf. Microw. Millim. Wave Technol.*, May 2010, pp. 769–771.

[13] R. Lian, Z. Wang, Y. Yin, J. Wu, and X. Song, "Design of a low-profile dual-polarized stepped slot antenna array for base station," *IEEE Antennas Wireless Propag. Lett.*, vol. 15, pp. 362–365, 2016.

[14] Y. He and Y. Yue, "A novel broadband dual-polarized dipole antenna element for 2G/3G/LTE base stations," in *Proc. IEEE Int. Conf. RFID Technol. Appl.*, Sep. 2016, pp. 102–104.
[15] Q. Liu and B. Liu, "Ultra wideband radiation element and its base station antenna for mobile communication," China Patent CN 204 966 674 U, Jan. 13, 2016.
[16] W. T. Joines, "A continuously variable dielectric phase shifter," *IEEE Trans. Microw. Theory Techn.*, vol. MTT-19, no. 8, pp. 729–732, Aug. 1971.
[17] M. Hassan and N. Karmaker, "Comparative study of different power distribution methods for array antenna beamforming for soil moisture radiometer," in *Proc. IEEE 11th Int. Conf. Sens. Technol.*, Dec. 2017, pp. 1–4.
[18] J. Zhou, K. A. Morris, and M. J. Lancaster, "General design of multiway multisection power dividers by interconnecting two-way dividers," *IEEE Trans. Microw. Theory Techn.*, vol. 55, no. 10, pp. 2208–2215, Oct. 2007.
[19] A. Tiwari, U. Pattapu, and S. Das, "A wideband 1: 2 T-junction power divider for antenna array with optimum results," in *Proc. Int. Conf. Microw. Photon.*, Feb. 2018, pp. 1–2.

YEJUN HE (SM'09) received the Ph.D. degree in information and communication engineering from Huazhong University of Science and Technology, Wuhan, China, in 2005. From 2005 to 2006, he was a Research Associate with the Department of Electronic and Information Engineering, Hong Kong Polytechnic University, Hong Kong. From 2006 to 2007, he was a Research Associate with the Department of Electronic Engineering, Faculty of Engineering, The Chinese University of Hong Kong, Hong Kong. In 2012, he was a Visiting Professor with the Department of Electrical and Computer Engineering, University of Waterloo, Waterloo, ON, Canada. From 2013 to 2015, he was an Advanced Visiting Scholar (Visiting Professor) with the School of Electrical and Computer Engineering, Georgia Institute of Technology, Atlanta, GA, USA. Since 2011, he has been a Full Professor with the College of Information Engineering, Shenzhen University, Shenzhen, China, where he is currently the Director of the Guangdong Engineering Research Center of Base Station Antennas and Propagation, and also the Director of Shenzhen Key Laboratory of Antennas and Propagation, Shenzhen, China. He has authored or coauthored over 110 research papers, books (chapters). He holds about 20 patents. His research interests include channel coding and modulation, 4G/5G wireless mobile communication, space-time processing, antennas and RF.

Dr. He is a fellow of IET. He is the IEEE Antennas and Propagation Society-Shenzhen Chapter Chair. He is currently serving as an Associate Editor of the IEEE Network, the IEEE Access, and the *International Journal of Communication Systems*. He has served as a Reviewer for various journals, such as the IEEE Transactions on Vehicular Technology, the IEEE Transactions on Communications, the IEEE Transactions on Wireless Communications, the IEEE Transactions on Industrial Electronics, the IEEE Wireless Communications, the IEEE Communications Letters, the *IEEE Journal on Selected Areas in Communications*, *International Journal of Communication Systems*, *Wireless Communications and Mobile Computing*, and *Wireless Personal Communications*. He has also served as a Technical Program Committee Member or the Session Chair for various conferences, including the IEEE Global Telecommunications Conference, the IEEE International Conference on Communications, the IEEE Wireless Communication Networking Conference, and the IEEE Vehicular Technology Conference. He is the Principal Investigator for over 20 current or finished research projects, including NSFC of China, the Integration Project of Production Teaching and Research by Guangdong Province and Ministry of Education, and the Science and Technology Program of Shenzhen City.

JUN LI received the B.S. degree in communication engineering from Shenzhen University, China, in 2016, where he is currently pursuing the master's degree with the College of Information Engineering. His research interests include base station antennas, mobile phone antennas, and radio frequency.

SAI WAI WONG (S'06–M'09–SM'14) received the B.S. degree in electronic engineering from The Hong Kong University of Science and Technology, Hong Kong, in 2003, and the M.Sc. and Ph.D. degrees in communication engineering from Nanyang Technological University, Singapore, in 2006 and 2009, respectively. From 2003 to 2005, he was the Lead of the Engineering Department in China, with two manufacturing companies in Hong Kong. From 2009 to 2010, he was a Research Fellow with the Institute for Infocomm Research, Singapore. Since 2010, he has been an Associate Professor and became a Full Professor with the School of Electronic and Information Engineering, South China University of Technology, Guangzhou, China. In 2016, he was a Visiting Professor with the City University of Hong Kong, Hong Kong. Since 2017, he has been a Full Professor with the College of Information, Shenzhen University, Shenzhen, China. His current research interests include RF/microwave circuit and antenna design. He was a recipient of the New Century Excellent Talents in University (NCET) Award in 2013 and the Shenzhen Overseas High-Caliber Personnel Level C in 2018. He is a Reviewer for several top-tier journals.

XIAOFANG PAN received the B.S. degree from Southeast University, Nanjing, China, in 2010, and the Ph.D. degree from The Hong Kong University of Science and Technology in 2015. She joined the College of Information Engineering, Shenzhen University, as an Assistant Professor. Her research activities are focused on electronic nose related fabrication, characterization, and algorithm analysis.

LONG ZHANG received the B.S. and M.S. degrees in electrical engineering from the Huazhong University of Science and Technology (HUST), Wuhan, China, in 2009 and 2012, respectively, and the Ph.D. degree in electronic engineering from the University of Kent, Canterbury, U.K, in 2017. He is currently an Assistant Professor with the College of Information Engineering, Shenzhen University, Shenzhen, China. His current research interests include circularly polarized antennas and arrays, mm-wave antennas and arrays, phased arrays, tightly coupled arrays, and reflect arrays. He served as a Reviewer for several technique journals, including the IEEE Transactions on Antennas and Propagation, the IEEE Antennas and Wireless Propagation Letters, the *IET Microwaves, Antennas and Propagation*, and the *Electronic Letters*.

ZHI NING CHEN (M'99–SM'05–F'07) received the B.Eng., M.Eng., and Ph.D. degrees from the Institute of Communications Engineering (ICE), China, and the second Ph.D. degree from the University of Tsukuba, Japan, respectively, all in electrical engineering.

From 1988 to 1995, he was a Lecturer and also an Associate Professor with ICE. He was a Post-Doctoral Fellow and also an Associate Professor with Southeast University, China. From 1995 to 1997, he joined The City University of Hong Kong as a Research Assistant and later a Research Fellow. From 1999 to 2016, he was with the Institute for Infocomm Research (I2R) as Principal Scientist, the Head of the RF and Optical Department, and the Technical Advisor. In 2012, he joined the Department of Electrical and Computer Engineering, National University of Singapore, as a tenured Full Professor, where he is currently the Program Director (Industry). He is holding/held the concurrent Guest Professorships at Southeast University (Changjiang Chair Professor), Nanjing University, Tsinghua University, Shanghai Jiaotong University, Tongji University, University of Science and Technology of China, Fudan University (Outstanding Visiting Professor), Dalian Maritime University, Chiba University, National Taiwan University of Science and Technology, Shanghai University (Ziqiang Professor), Beijing University of Posts and Telecommunications, Tohoku University, and the City University of Hong Kong (Adjunct Professor). He is holding 28 granted/ filed patents with 35 licensed deals with industry. He is interested in electromagnetic engineering and antennas/sensors for communication, radar, imaging, and sensing systems. He is a member of the State Key Laboratory of Millimeter-waves with Southeast University and the City University of Hong Kong. In 1997, he was a recipient of the Japan Society for the Promotion of Science (JSPS) Fellowship to conduct his research at the University of Tsukuba, Japan. He is a recipient of the International Symposium on Antennas and Propagation Best Paper Award 2010, the CST University Publication Awards 2008 and 2015, the ASEAN Outstanding Engineering Achievement Award 2013, the Institution of Engineers Singapore Prestigious Engineering Achievement Awards 2006, 2013(2), and 2014, the I2R Quarterly Best Paper Award 2004, the IEEE iWAT 2005 Best Poster Award, several technology achievement awards from China from 1990 to 1997, as well as over 19 academic awards by the students he supervised. He is the founding General Chairs of the International Workshop on Antenna Technology (iWAT) in 2005, the International Symposium on InfoComm and Mechatronics Technology in Bio-Medical and Healthcare Application (IS 3Tin3A) in 2010, the International Microwave Forum (IMWF) in 2010, and the Asia-Pacific Conference on Antennas and Propagation (APCAP) in 2012. He has also involved in many international events as the General Chairs, Chairs, and members for technical program committees and international advisory committees. He has published over 580 academic papers and five books entitled *Broadband Planar Antennas* (Wiley, 2005), *UWB Wireless Communication* (Wiley, 2006), *Antennas for Portable Devices* (Wiley, 2007), *Antennas for Base Stations in Wireless Communications* (McGraw-Hill, 2009), and Handbook of Antenna Technologies with 76 chapters (Springer References, 2016), as an Editor-in-Chief. He has also contributed the chapters to the books entitled *UWB Antennas and Propagation for Communications, Radar, and Imaging* (Wiley, 2006), *Antenna Engineering Handbook* (McGraw-Hill, 2007), *Microstrip and Printed Antennas* (Wiley, 2010), and *Electromagnetics of Body Area Networks* (Wiley, 2016).

Dr. Chen was elevated as a fellow of the IEEE for the contribution to small and broadband antennas for wireless applications in 2007. Since 2015, he has been serving for the IEEE Council on RFID as a Vice President and a Distinguished Lecturer. He was an Associate Editor of the IEEE TRANSACTION ON ANTENNAS AND PROPAGATION and also a Distinguished Lecturer for the IEEE ANTENNAS AND PROPAGATION SOCIETY.